



Spironolactone inhibits endothelial-mesenchymal transition via the adenosine A2A receptor to reduce cardiorenal fibrosis in rats

Xingxing Chen^{a,1}, Wenhua Ge^{b,1}, Tiancheng Dong^a, Jie Hu^a, Lingzhi Chen^c, Xiaofang Fan^d, Yongsheng Gong^{d,*}, Hao Zhou^{a,*}

^a Department of Cardiology, the First Affiliated Hospital of Wenzhou Medical University, Wenzhou 325000, China

^b Stomatological Hospital, College of Medicine, Xi'an Jiaotong University, Xi'an 710004, China

^c Department of Clinical laboratory, Wenzhou Central Hospital, Wenzhou 325000, China

^d Department of Hypoxia Medical Research Laboratory, Wenzhou Medical University, Wenzhou 325000, China

ARTICLE INFO

Keywords:

Spironolactone
Endothelial-mesenchymal transition
Fibrosis
Adenosine A2A receptor
Cardiorenal syndrome

ABSTRACT

Aims: The mechanisms underlying cardiorenal syndromes are complex and not fully understood; Fibrosis seems to be a primary driver of the diseases' pathophysiology. Spironolactone can reduce cardiac or renal fibrosis by inhibiting endothelial-mesenchymal transition (EndMT). Spironolactone protection may rely on activation of adenosine receptors, but the role of the adenosine A2A receptor (A2AR) is unclear. We hypothesize that spironolactone may modulate A2AR to suppress EndMT and reduce cardiorenal remodeling.

Main methods: A model of renal injury followed by heart failure was established by subcutaneous administration of isoprenaline (Iso) to rats. Assessment of cardiac and renal function, fibrosis, EndMT markers, adenosine and A2AR expression was performed. TGF- β was used to induce EndMT in primary human umbilical vein endothelial cells (HUVECs). Rats or cells were divided into four groups: those that treated with spironolactone alone or in combination with A2AR antagonist ZM241385 or neither, and compared to normal controls.

Key findings: Isoprenaline-treated rats exhibited cardiac and renal fibrosis, impaired cardiac and renal function, enhanced EndMT, and lower A2AR expression. Spironolactone significantly up-regulated A2AR expression and inhibited EndMT in vivo and in vitro. Moreover, spironolactone improved cardiorenal remodeling and reduced dysfunction. These changes were exacerbated by administration of ZM241385. Together, these findings show that spironolactone up-regulated A2AR to reduce EndMT and ameliorate cardiorenal fibrosis.

Significance: The anti-fibrotic effects of spironolactone may partly depend on the up-regulation of A2AR, and that A2AR might be a potential therapeutic target for the treatment of cardiorenal syndrome.

1. Introduction

Cardiorenal syndromes (CRS) are widely defined as conditions in which acute or chronic dysfunction of either the heart or kidney may induce acute or chronic failure of the other [1]. The coexistence of kidney and heart failure carries an extremely bad prognosis. The severity of renal dysfunction is independently associated with worse outcomes in patients with chronic heart failure during their mid-term follow-up [2]. In a RELAX-AHF trial, administration of serelaxin (recombinant human relaxin-2, a potent renal vasodilator [3]), lowered all-cause mortality in patients of decompensated heart failure after 180 days [4]. Moreover, this improvement in overall clinical outcome was most likely because of the highly significant increase in glomerular

filtration rate in response to serelaxin [5].

Despite decades of clinical research and innovations in the treatment of cardiorenal syndrome, it remains a leading global health problem because of unclear pathogenesis. Fibrosis is thought to be a critical participant in the pathophysiology of increased CRS risk [6]. In a 5/6 nephrectomy of rats following myocardial infarction (a typical CRS model), investigators found increased interstitial cardiac fibrosis and collagen type I expression in the non-infarct myocardium and increased renal tubulointerstitial fibrosis [7]. The renin-angiotensin-aldosterone system (RAAS) is a pivotal cardiorenal connector, because it satisfies the prerequisite of a bidirectional response and can be initiated by both heart failure and renal failure. Activation of the RAAS will culminate in tissue remodeling and fibrosis [8].

* Corresponding authors.

E-mail addresses: fxbwzmc@126.com (Y. Gong), wyzh66@126.com (H. Zhou).

¹ These authors contributed equally to this work.

Accumulating evidence shows that spironolactone, a mineralocorticoid receptor (MR) antagonist, plays a protective role in cardiac and renal diseases, but its role in cardiorenal syndrome remains obscure. Spironolactone improves heart failure by reducing cardiac fibrosis [9] and also decreases collagen deposition and exhibits direct renoprotective effects in diabetic rats [10]. Recently, Calvier et al. found aldosterone-induced cardiac and renal fibrosis and dysfunction as well as renal epithelial-mesenchymal transition (EMT) in rats were reversed by spironolactone [11]. Our previous study demonstrated that spironolactone alleviated cardiac fibrosis via inhibition of endothelial-mesenchymal transition (EndMT, a process similar to EMT) [12], which has been accepted as a novel mechanism for organ fibrosis and is widely researched [13–16]. The aforementioned studies indicate that spironolactone may attenuate CRS via EndMT modulation.

Animal studies showed that the cardioprotective effect of the MR antagonist, canrenoate, was abrogated in adenosine receptor knock-out mice [17], indicating that the protection of MR antagonists may rely on activation of adenosine signaling.

Adenosine is an endogenous regulator of inflammation and tissue repair. The effects of extracellular adenosine are mediated by four G-protein coupled adenosine receptors (A1R, A2AR, A2BR, and A3R) [18]. Adenosine and A2AR are related to the progression of fibrosis in various organs, including cardiac and renal fibrosis [19–21]. In obstructive nephropathy, A2AR activation alleviated deposition of collagen types I and III by suppressing epithelial-mesenchymal transition [22].

However, it is unknown whether A2AR is associated with EndMT in CRS. The aim of the current study was to investigate whether spironolactone influences A2AR expression, thereby modulating EndMT and cardiorenal fibrosis.

2. Materials and methods

2.1. Animals and treatments

All experiments and procedures were approved by the Institutional Research Ethics Committee of Wenzhou Medical University and were in accordance with the National Institutes of Health Guide for the Care and Use of Laboratory Animals. Male Sprague-Dawley rats (approximately 6-week-old) were purchased from the Wenzhou Medical University Laboratory Animal Center. Rats were randomly assigned to four treatment groups (n = 10 per group): (1) control; (2) Iso (isoprenaline 5 mg/kg/day for 7 days, single injection); (3) Iso (5 mg/kg/day) for 7 days + spironolactone (60 mg/kg/day) for 21 days, and (4) Iso (5 mg/kg/day) for 7 days + spironolactone (60 mg/kg/day) for 21 days + ZM241385 (3 mg/kg/day) for 21 days. Rats were subcutaneously injected with Iso (Sigma, St. Louis, MO, USA) to induce heart failure. Control rats were administered saline in the same way. Beginning on day 1, rats in the medication groups were gavaged daily with spironolactone (H33020070, Minsheng Pharma, Hangzhou, China) for 21 consecutive days, and the non-drug groups were gavaged with the same volume of saline. A selective A2AR antagonist, ZM 241385 (intraperitoneal administration, 1 h prior to spironolactone), was purchased from Tocris Cookson (Ballwin, MO, USA). At day 22, rats were randomly chosen for echocardiography and hemodynamic testing. All animals were then euthanized and the heart and kidney tissues were harvested.

2.2. Echocardiographic study

Rats were anaesthetized with sodium pentobarbital (40 mg/kg, intraperitoneal) and placed on a heating pad. Cardiac function was detected using a Sonos 5500 ultrasound machine (Phillips, USA). The transducer covered with ultrasound transmission gel was used at a depth setting of 2 cm for optimum resolution. Two-dimensional, M-mode images were captured in parasternal long-axis view to measure

left ventricular end-diastolic diameter (LVEDD). Ejection fraction (EF) and fractional shortening (FS) were then calculated.

2.3. Hemodynamic testing

Rats were weighed and anaesthetized via an intraperitoneal injection of 1% sodium pentobarbital (40 mg/kg). The left ventricle (LV) was catheterized to monitor changes in left ventricle end diastolic pressure (LVEDP), LV mean systolic pressure (LVSP), and maximum rate of change in LV pressure (+ dp/dtmax, - dp/dtmax) via the right common carotid artery.

2.4. Organ weight index and serum creatinine measurement

Rats were humanely euthanized, then pre-cooled saline (4 °C) was infused into the left ventricle until the heart and kidney became pale. The left and right ventricles were separated and weighed. Left ventricle weight indices (LVWI) were calculated as free wall mass (mg) of left ventricles/body mass (g). Kidney mass index (KWI) was computed as the average of the two kidneys (mg)/body mass (g). Serum creatinine (SCr) was measured using a 7180 automatic biochemical analyzer (Hitachi High-Technologies Corp., Japan).

2.5. Hematoxylin and eosin staining

Ventricle and kidney samples were embedded in paraffin and sectioned. Paraffin sections (4 μm thick) were stained with hematoxylin and eosin. Sections were examined by light microscopy and photographed at ×200 magnification.

2.6. Masson trichrome staining

Paraffin sections were stained with Masson trichrome (G1340, Solarbio Life Sciences Beijing, China), then examined by light microscopy and photographed at ×200 magnification. Fibrous tissue stained blue, cytoplasm red, and cell nuclei black.

2.7. Quantification of adenosine levels by UPLC-MS/MS analysis

The levels of adenosine in heart and kidney were quantified using an ultra-performance liquid chromatography-mass spectrometry system (ACQUITY UPLC system; Waters) and a tandem mass spectrometry system (AB SCIEX Triple Quad™ 5500 System) (UPLC-MS/MS) as previously described [23]. In brief, 3 μl of sample was injected and separated by a BEH UPLC C18 column (100 mm × 2.1 mm, 1.7 μm). The mobile phase composition was: (A) pure water + 0.1% formic acid (v/v), (B) pure acetonitrile; flow rate was 0.4 ml/min; column temperature was 40 °C; gradient separation conditions were as follows: 0–0.5 min, 1% B; 1.0 min, 15% B; 2.5 min, 30% B; 2.5–4.0 min, 100% B; 4.0–5.5 min, 1% B. Electrospray ionization (ESI) was used in positive mode for detection of the eluents. MS conditions were as follows: Source temperature: 600 °C, curtain gas (CUR): 25 psi, ion source gas 1 (GAS 1): 50 psi, ion source gas 2 (GAS2): 50 psi, collision gas (CAD): 8 psi, ion spray voltage (IS): 5500 V, entrance potential (EP): 10 V, collision cell exit potential (CXP1): 14 V. The qualitative and quantitative detection of metabolites were performed by multiple-reaction monitoring (MRM). Then we used the software Analyst® (version 1.5.2, AB Sciex) for data collection and analysis.

2.8. Enzyme-linked immunosorbent assay

A piece of kidney (100 mg) was cut into pieces and added to 1 ml phosphate-buffered saline (PBS, pH 7.4) on ice and then homogenized. The homogenate was centrifuged at 3000 rpm for 20 min, the supernatant recovered, and the amount of collagen types I and III determined using an enzyme-linked immunosorbent assay (ELISA) kit (Shanghai

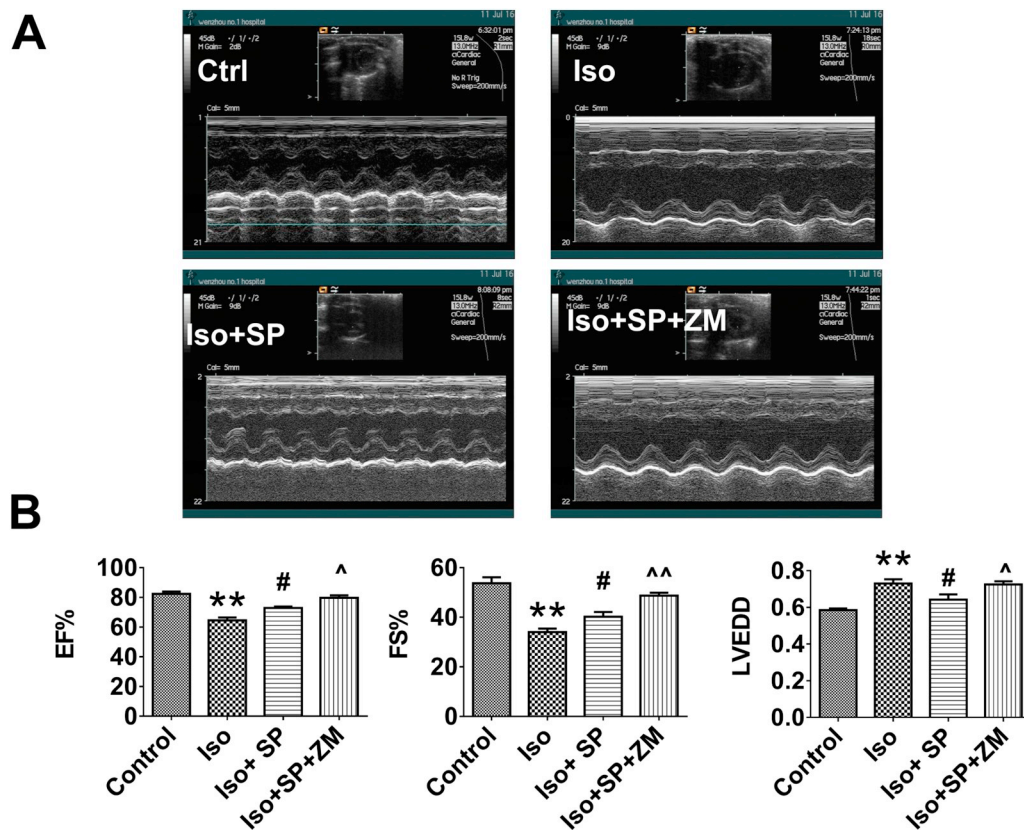


Fig. 1. Echocardiographic assessment of cardiac function, $n = 4$. (A) Representative echocardiographic photos from M-mode. (B) Analysis of cardiac dimension (LVEDd, left ventricular end-diastolic internal diameters) and cardiac pump function (EF%, ejection fraction; FS%, fractional shortening). Data are mean \pm standard deviation. ** $P < 0.01$ vs. Control; # $P < 0.05$ vs. Iso; $P < 0.05$, ^ $P < 0.01$ vs. Iso + SP. Iso, isoprenaline; SP, spironolactone; ZM, ZM241385.

Boyun Biotech, China) according to the manufacturer's instructions.

2.9. Cell culture

Primary human umbilical vein endothelial cells (HUVECs) were purchased from the cell bank of the Chinese Academy of Science (Shanghai, China). Cells were cultured in DMEM (Lonza, USA) with 10% fetal bovine serum (FBS, Gibco, USA), 100 U/ml penicillin (Gibco), and 100 mg/ml streptomycin (Gibco). All cells were maintained at 37 °C in a 5% CO₂ incubator. Cells were randomly grouped according to different treatments: (1) control; (2) TGF- β ; (3) TGF- β + spironolactone; (4) TGF- β + spironolactone + ZM241385. Cells were pre-treated with spironolactone (1 μ M) for 2 h before incubation with TGF- β (10 ng/ml) for another 24 h. ZM241385 (50 nM) was administered 1 h before spironolactone treatment.

2.10. Immunofluorescence assay

Sections of LV myocardium and kidney tissues were treated with 3% methanol-H₂O₂ to block endogenous peroxidase activity, and non-specific sites were blocked with 10% fetal bovine serum. Sections were incubated with primary antibodies (anti-CD31, ab28364; anti-VE-cadherin, ab33168; anti- α -SMA, ab5694; anti-vimentin, ab92547, all from Abcam, Cambridge, 1:1000) at 4 °C overnight. After washing with PBS (3 washes, 5 min per wash), sections were incubated with secondary antibodies for 1 h, then incubated with DAPI staining solution for 5 min to stain nuclei. Photographs were taken at $\times 200$ magnification. Negative control sections were incubated with PBS only and showed no positive staining. Sections incubated with suitable isotype control primary antibodies, and fluorescent-labeled secondary antibodies were also used as negative controls.

2.11. Western blot analysis

Left ventricular myocardium and kidney tissues were lysed in RIPA buffer and then centrifuged at 12,000 rpm for 10 min at 4 °C. Supernatant was collected, and protein concentrations were determined using a bicinchoninic acid (BCA) protein assay (PC0020, Solarbio Life Sciences Beijing, China). Equal amounts of each sample (80 μ g) were separated by SDS-PAGE and transferred onto polyvinylidene fluoride membranes. Membranes were blocked with 5% skimmed milk and incubated with primary antibodies (anti-adenosine receptor A2a, ab3461; anti-CD31, ab28364; anti-VE-cadherin, ab33168; anti- α -SMA, ab5694; anti-vimentin, ab92547, all from Abcam, Cambridge, 1:1000) overnight at 4 °C. Membranes were washed three times with PBST, followed by incubation with a horseradish peroxidase-conjugated secondary antibody. Scans were obtained using a Bio-Rad gel image analysis system (BioRad, Hercules, CA, USA) and analyzed using the ImageJ processing program.

2.12. Quantitative Real-Time PCR

Total RNA was extracted from LV myocardium and kidney samples using Trizol reagent (139505, Life Technologies, UK) then reverse transcribed to cDNA using a RevertAid First Strand cDNA Synthesis Kit (K1622, Thermo Scientific, Germany), according to the manufacturer's instructions. qPCR was performed to quantify the expression level of A2AR and glyceraldehyde 3-phosphate dehydrogenase (GAPDH) using SYBR GreenER™ qPCR SuperMix Universal (1608533, Life Technologies, UK). PCR conditions consisted of an initial step at 95 °C (5 min), followed by 40 cycles of denaturation at 95 °C (15 s) and annealing at 60 °C (1 min). All samples were amplified in duplicate, and each experiment was repeated independently three times. The PCR primers for rat were as follows: A2AR: F-5'-TCGTGGAGTCCCGTCTT TCT-3' and R-5'-GCCCTCTCTTCGCTGTTTG-3'; GAPDH: F-5'-TCTCT GCTCCTCCTGTTTC-3' and R-5'-ACACCGACCTTCACCATCT-3'.

Table 1
Hemodynamic testing of cardiac functional index.

| Group | No | LVSP/mm Hg | LVEDP/mm Hg | +dp/dt/mm Hg/s | −dp/dt/mm Hg/s |
|---------------|----|-----------------------------------|---------------------------------|---------------------------------|----------------------------------|
| Control | 8 | 135.7 ± 23.4 | −4.9 ± 0.2 | 9065.8 ± 581.8 | −7959.3 ± 655.7 |
| Iso | 8 | 101.4 ± 13.2 ^{**} | 18.9 ± 0.9 ^{**} | 3384.2 ± 161.2 ^{**} | −3109.3 ± 565.4 ^{**} |
| Iso + SP | 8 | 131.4 ± 4.6 ^{##} | −1.1 ± 0.2 ^{##} | 6309.8 ± 839.6 ^{##} | −5559.2 ± 1102.5 ^{##} |
| Iso + SP + ZM | 8 | 121.0 ± 3.1 ^{&&} | 9.5 ± 0.5 ^{&&} | 5034.2 ± 982.7 ^{&} | −4407.8 ± 519.2 ^{&} |

Data are shown as mean ± standard deviation. Iso, isoprenaline; SP, spironolactone; ZM, ZM241385.

^{**} P < 0.01 vs. Control.

^{##} P < 0.01 vs. Iso.

[&] P < 0.05 vs. Iso + SP.

^{&&} P < 0.01 vs. Iso + SP.

Table 2
Organ weight index and renal function.

| Group | Body weight (g) | LVWI (mg/g) | KWI (mg/g) | SCr (μmol/L) |
|---------------|--------------------------------|-----------------------------------|------------------------------|-------------------------------|
| Control | 266.9 ± 16.4 | 2.39 ± 0.22 | 3.71 ± 0.54 | 26.83 ± 5.17 |
| Iso | 212.4 ± 18.6 ^{**} | 3.19 ± 0.22 ^{**} | 4.71 ± 0.45 ^{**} | 34.58 ± 5.70 [#] |
| Iso + SP | 254.1 ± 8.0 ^{##} | 2.54 ± 0.28 [#] | 3.94 ± 0.54 [#] | 27.85 ± 3.81 [#] |
| Iso + SP + ZM | 234.5 ± 15.12 ^{&} | 3.08 ± 0.32 ^{&&} | 4.67 ± 0.58 ^{&} | 34.33 ± 4.00 ^{&} |

Data are shown as mean ± standard deviation. N = 8 per group. LVWI: left ventricle weight indices; KWI: kidney mass index; SCr: serum creatinine.

^{*} P < 0.05 vs. Control.

^{**} P < 0.01 vs. Control.

[#] P < 0.05 vs. Iso.

^{##} P < 0.01 vs. Iso.

[&] P < 0.05 vs. Iso + SP.

^{&&} P < 0.01 vs. Iso + SP.

2.13. Statistical analysis

Data are represented as the mean ± SD and were analyzed using SPSS 19.0 software. One-way analysis of variance (ANOVA) was used to compare more than two groups. P < 0.05 was considered statistically significant.

3. Results

3.1. Spironolactone treatment improves cardiac pump function

Changes in cardiac function were assessed using echocardiography and hemodynamic testing. Representative M-mode echocardiograms are shown in Fig. 1A. As shown in Fig. 1B, EF and FS were lower, but LVEDD was significantly higher in Iso-treated rats compared with controls. Treatment with spironolactone increased EF and FS and decreased LVEDD compared with Iso treatment alone. However, ZM241385 lowered EF and FS and increased LVEDD. Consistently, hemodynamic results also showed a deterioration in cardiac function in fibrotic rats compared with controls. Spironolactone attenuated these Iso-induced changes in ventricular function, as evidenced by higher LVSP, +dp/dtmax and −dp/dtmax, and lower LVEDP. These changes were significantly reversed after administration of ZM241385 (Table 1). The data demonstrated that cardiac dysfunction in Iso-treated rats was improved after co-treatment with spironolactone, but that these cardioprotective effects were reversed by ZM241385.

3.2. Spironolactone decreased LVWI and KWI and inhibited renal injury

Compared with controls, Iso treatment significantly increased LVWI, KWI, and SCr, and reduced body weight. Spironolactone treatment resulted in lower LVWI, KWI, and SCr and higher body weight, while co-treatment with ZM241385 significantly increased LVWI, KWI, SCr and decreased body weight (Table 2).

3.3. Spironolactone mitigates cardiorenal fibrosis and collagen deposition

Hematoxylin and eosin and Masson trichrome staining showed that heart and kidney tissues from Iso-treated rats exhibited collagen fiber hyperplasia, irregular morphology, and leukocyte infiltration compared with the controls (Fig. 2A, B). ELISA results also showed higher levels of collagen type I and III in Iso-treated heart and kidney (Fig. 2C). Spironolactone administration reduced the degree of fibrous hyperplasia and the deposition of collagen I/III. The ratio of collagen I/III was increased in the Iso group and decreased in the spironolactone group. Compared with the spironolactone group, these changes were reversed by co-administration of ZM241385 (Fig. 2).

3.4. Spironolactone reduces EndMT in vivo and in vitro

Immunofluorescence staining and western blot analysis were used to detect the expression of EndMT markers, including cluster of differentiation-31 (CD31), vascular endothelial-cadherin (VE-cadherin), α-smooth muscle actin (α-SMA) and vimentin. Compared with the control group, levels of α-SMA and vimentin were higher, but the expression of CD31 and VE-cadherin was lower in the Iso group, indicating the occurrence of EndMT. Spironolactone treatment significantly inhibited EndMT by increasing CD31 and VE-cadherin expression, and by decreasing α-SMA and vimentin levels. Importantly, co-treatment with ZM241385 promoted EndMT compared with the spironolactone group (Figs. 3, 4).

Similarly, in HUVECs, TGF-β induced EndMT as evidenced by increased levels of α-SMA and decreased levels of CD31. Spironolactone significantly reduced EndMT by increasing CD31 and decreasing α-SMA levels. Co-treatment with ZM241385 reversed EndMT (Fig. 5).

3.5. Spironolactone up-regulated adenosine A2AR to suppress EndMT

To investigate the role of A2AR during EndMT, we examined mRNA and protein levels of A2AR in cardiac and renal tissues. We found that A2AR expression was reduced in the Iso group compared with controls.

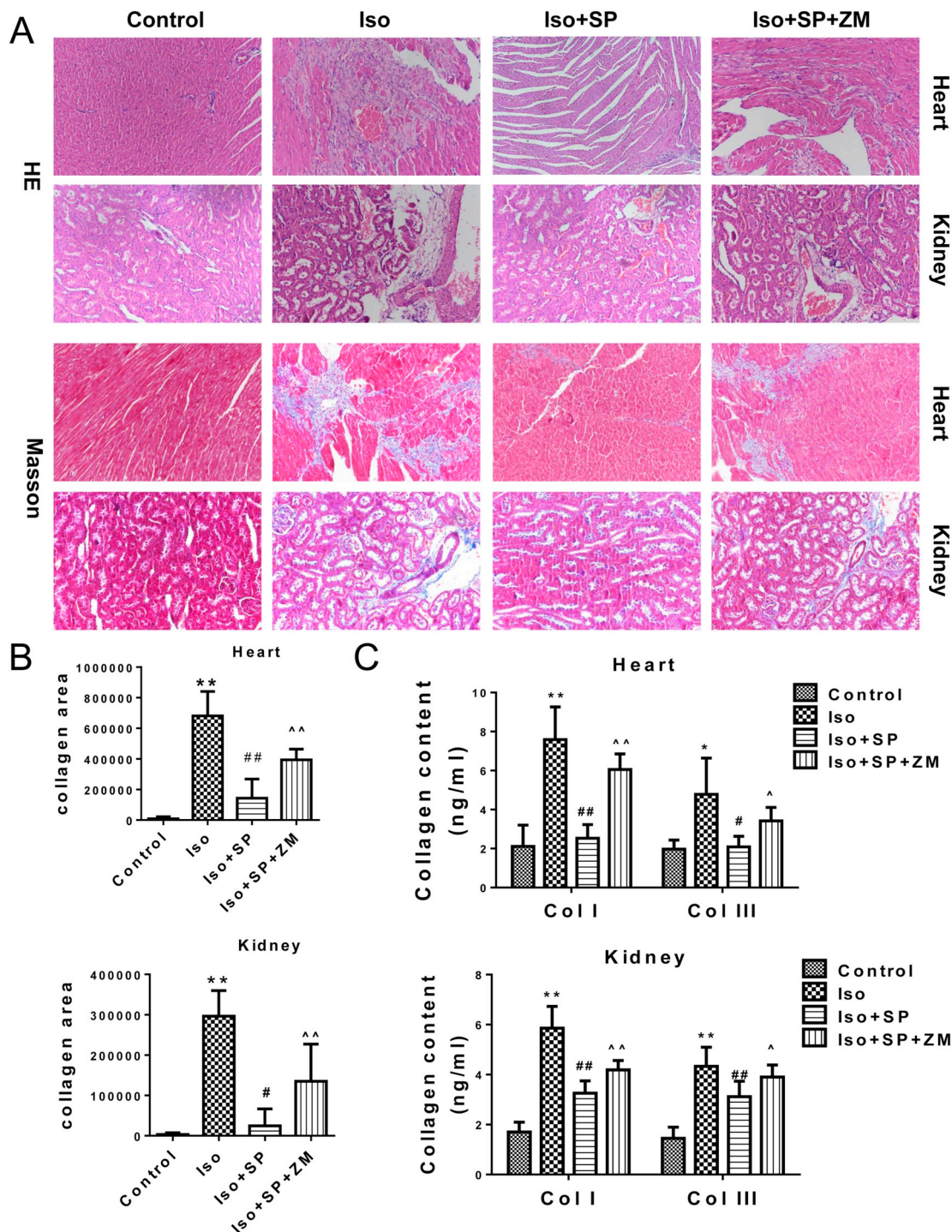


Fig. 2. Spironolactone reduces cardiac and renal fibrosis. (A) Hematoxylin and eosin staining & Masson staining of the heart and kidney tissues of rats, Magnification $\times 20$, $n = 5$. (B) Analysis of collagen area according to Masson staining. (C) ELISA analysis of collagen types I and III, $n = 4-6$. Data are shown as mean \pm standard deviation. * $P < 0.05$, ** $P < 0.01$ vs. Control; # $P < 0.05$, ## $P < 0.01$ vs. Iso; ^ $P < 0.05$, ^^ $P < 0.01$ vs. Iso + SP. Col I: collagen type I; Col III: collagen type III.

However, no significant difference was found in cardiac and renal adenosine levels (Fig. 6C, Table 3). Spironolactone resulted in higher expression of A2AR compared with the Iso group. A2AR mRNA and protein levels were lower in the ZM241385 treatment group compared with the spironolactone group (Fig. 6A, B).

4. Discussion

In the present study, Iso-treated rats exhibited cardiac and renal

fibrosis, enhanced EndMT, and lower A2AR expression. Spironolactone increased A2AR expression, inhibited EndMT, improved cardiorenal remodeling and reduced cardiac dysfunction. These changes were reversed by administration of the A2A antagonist, ZM241385. These data support our hypothesis that spironolactone stimulates A2AR to inhibit EndMT in the process of cardiorenal fibrosis.

Cardiorenal syndromes form a complex disease with multifactorial pathophysiology, such as over-activation of the renin-angiotensin-aldosterone system (RAAS), inflammation and oxidative stress [24].

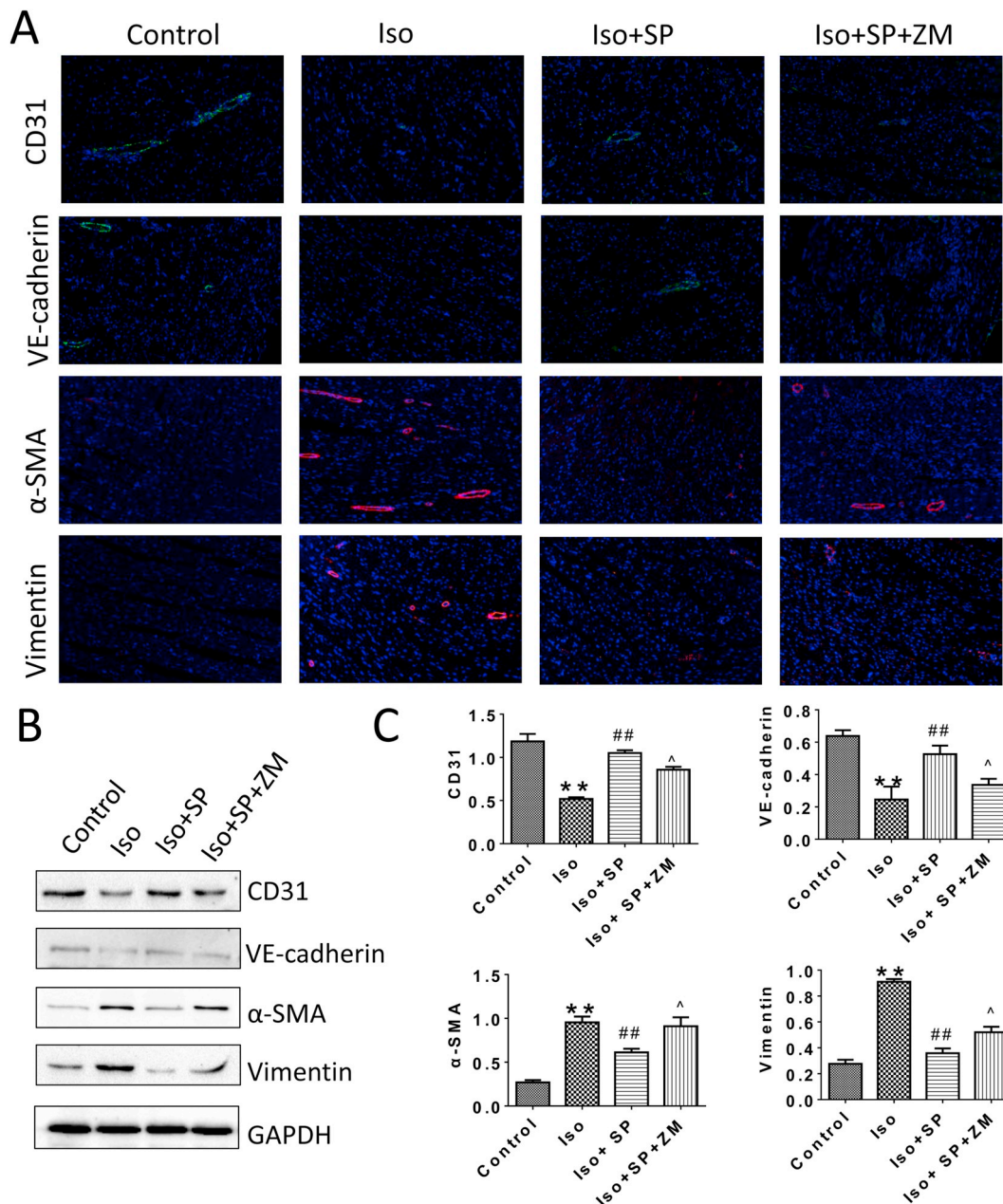


Fig. 3. Spironolactone inhibits EndMT in heart. (A) Immunofluorescence staining of EndMT markers. CD31, VE-cadherin protein (endothelial marker) are stained in green. α-SMA, Vimentin protein (myofibroblastic marker) are stained in red. Nuclei are stained with DAPI (blue). Magnification × 20, n = 6. (B–C) Protein expression of CD31, VE-cadherin, α-SMA, and vimentin by western blotting, n = 6. **P < 0.01 vs. Control; ##P < 0.01 vs. Iso; ^P < 0.05 vs. Iso + SP. (For interpretation of the references to color in this figure legend, the reader is referred to the web version of this article.)

RAAS activation by renal hypoperfusion stimulates the sympathetic nervous system and triggers a cascade of mechanisms that result in fibrosis in the heart, kidneys and vessels, and may reciprocally evolve into a cardiorenal syndrome. Whether in the heart or in the kidney, fibrosis is the common consequence of inflammation- and oxidative stress-linked endothelial dysfunction that leads to heart failure and chronic kidney disease [25]. Some researchers suggest that cardiac and renal fibrosis may act as a primary driver in the pathogenesis and progression of cardiorenal syndromes [6].

Fibroblasts, the most important effector cells in fibrosis, produce collagen proteins to form the extracellular matrix [13]. In addition to the resident fibroblast, activated fibroblasts or myofibroblasts can also

be derived from the transdifferentiation of endothelial cells, a process named EndMT, which features the loss of endothelial cell markers, such as CD31 and VE-cadherin, and acquisition of mesenchymal markers, like α-SMA and vimentin [15].

In our model, subcutaneous injection of Iso induced cardiac and renal injury as evidenced by increased serum creatinine, damaged cardiac function and diffuse collagen deposition. We observed EndMT in cardiac and renal tissues of Iso-treated rats, as indicated by elevated expression of CD31 and VE-cadherin and reduced expression of α-SMA and vimentin. Interestingly, these aforementioned changes were abolished by spironolactone treatment. In other words, spironolactone inhibits the Iso-induced EndMT process and attenuates cardiorenal

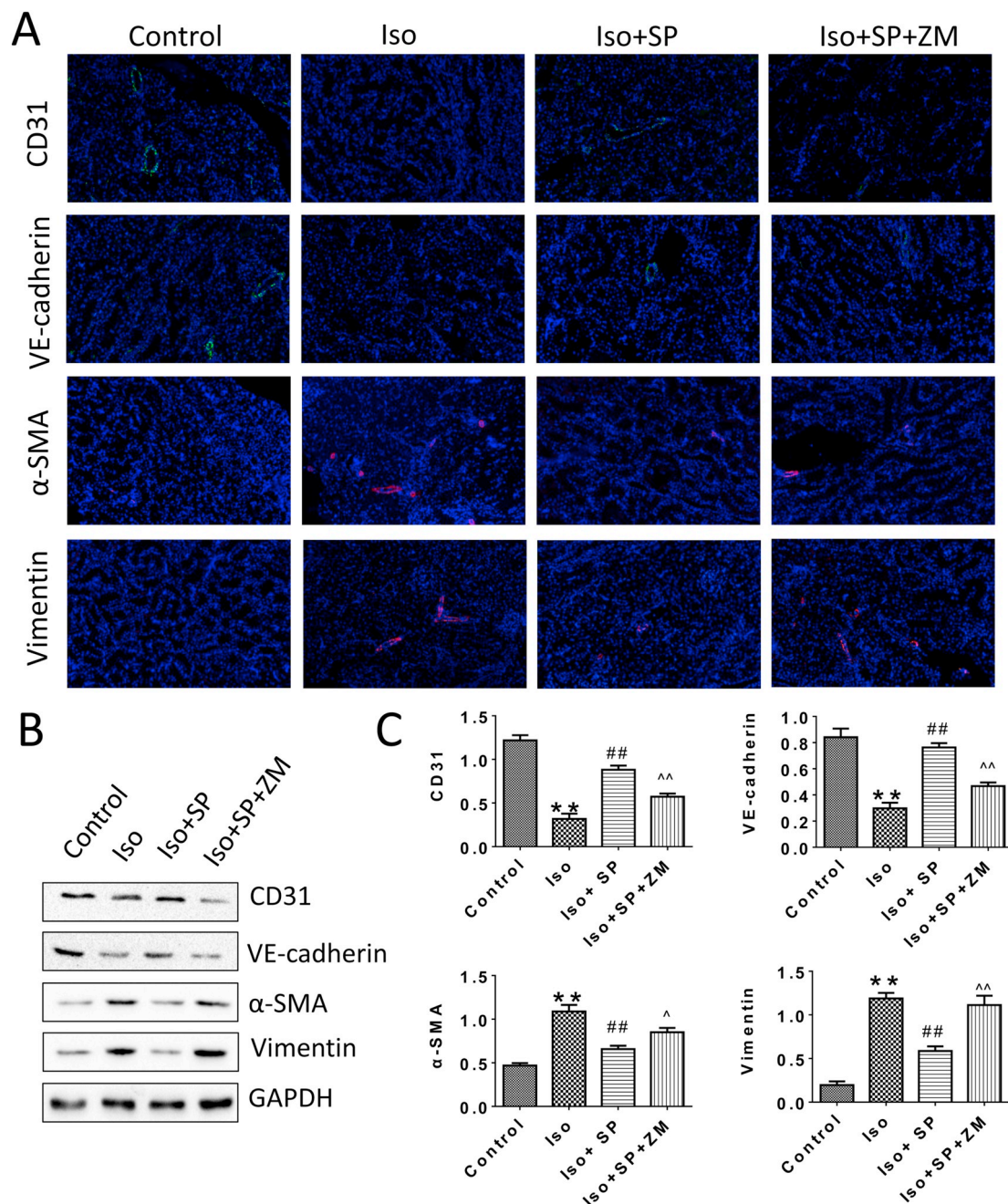


Fig. 4. Spironolactone inhibits EndMT in kidney. (A) Immunofluorescence staining of EndMT markers. CD31, VE-cadherin protein (endothelial marker) are stained in green. α -SMA, Vimentin protein (myofibroblastic marker) are stained in red. Nuclei are stained with DAPI (blue). Magnification $\times 20$, $n = 6$. (B–C) Protein expression of CD31, VE-cadherin, α -SMA, and vimentin by western blotting, $n = 6$. ** $P < 0.01$ vs. Control; ## $P < 0.01$ vs. Iso; $\tilde{P} < 0.05$, $\hat{P} < 0.01$ vs. Iso + SP. (For interpretation of the references to color in this figure legend, the reader is referred to the web version of this article.)

fibrosis and dysfunction.

Spironolactone, a high-affinity but nonspecific mineralocorticoid receptor antagonist that has structural similarity to progesterone, is commonly used clinically as a diuretic to relieve edema [26]. Clinical trials have reported a survival benefit of mineralocorticoid receptor antagonist treatment in patients with heart failure [27]. Schmidt and his colleagues demonstrated that adenosine receptor stimulation appeared to be critical for mineralocorticoid receptor antagonist-induced cardio-protection [17]. The nonspecific adenosine receptor antagonist, 8-*p*-sulphophenyltheophylline, completely abolished the protective

effect of eplerenone, a [steroidal anti-mineralocorticoid](#) of the [spironolactone](#) group, in isolated perfused rat hearts [17], indicating that the underlying mechanism of mineralocorticoid receptor antagonist benefits may depend on adenosine receptor activation.

It has been previously reported that adenosine, acting through A2AR, inhibits tissue fibrosis. For instance, the A2AR agonist CGS21680 effectively arrested lung inflammation to inhibit pulmonary fibrosis [28]. These studies support the anti-fibrotic action of A2AR activation. The A2AR-mediated increases in collagen synthesis are mainly achieved by activation of the cAMP-PKA or cAMP-Epac signaling pathway

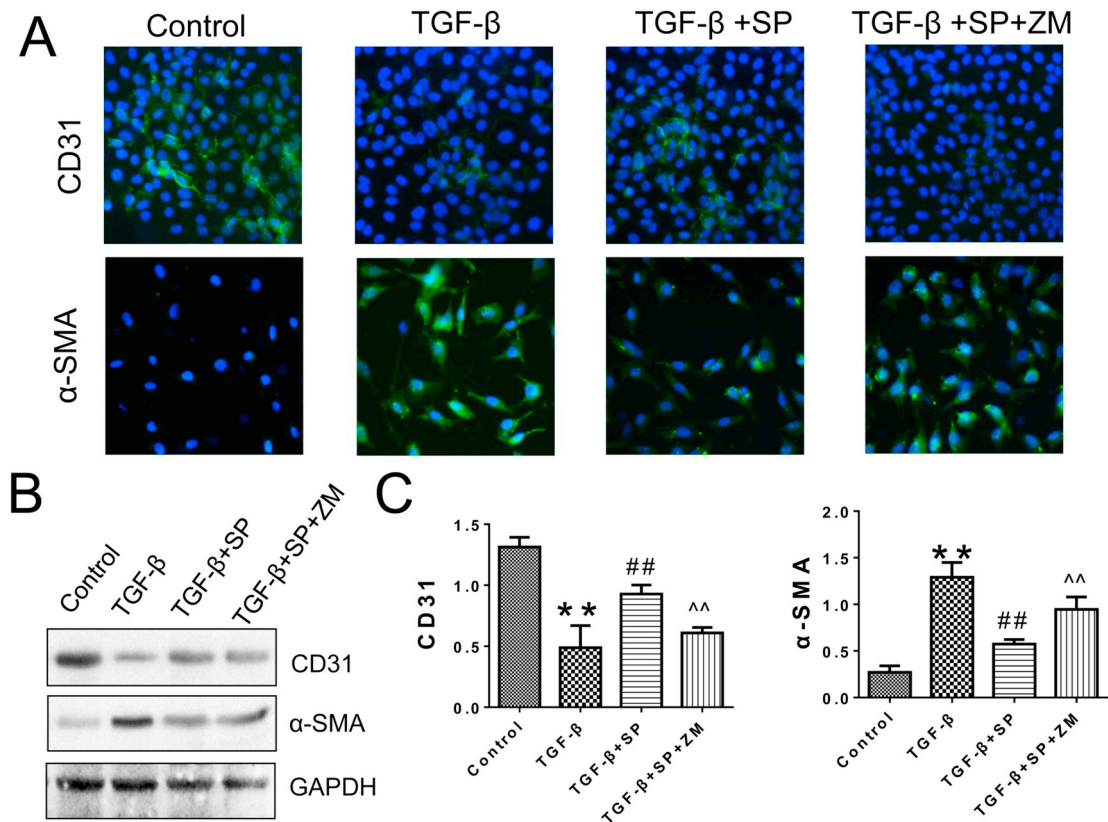


Fig. 5. Spironolactone reduces EndMT in HUVECs. (A) Immunofluorescence staining of EndMT markers. Magnification $\times 20$. Red, α -SMA; green, CD31; nucleus, blue. (B–C) Protein expression of CD31, VE-cadherin, α -SMA, and vimentin by western blotting, $n = 4-6$. ** $P < 0.01$ vs. Control; ## $P < 0.01$ vs. Iso; ^^ $P < 0.01$ vs. Iso + SP. (For interpretation of the references to color in this figure legend, the reader is referred to the web version of this article.)

[29,30]. Furthermore, in renal tubular epithelial cells, A2AR stimulation with CGS21680 reduced TGF β 1-induced EMT, while the A2AR selective antagonist, ZM241385, reversed the agonist-mediated effects, both of which are enacted through the cAMP-PKA or cAMP-MAPK/ERK axis [31].

In accordance with previous studies, our study also found that A2AR expression, not adenosine, was obviously decreased in the Iso treatment group compared with controls, while spironolactone treatment resulted in elevated A2AR expression accompanied by reduced EndMT. Spironolactone also significantly alleviated cardiorenal collagen deposition, and improved cardiac output and renal function. A2AR modulates the balance of collagen I: collagen III, so that the collagen I/III ratio decreases as A2AR activation increases [32]. Hence, the decline of the collagen I/III ratio in the spironolactone group also indirectly reflects A2AR activation. These changes were then reversed in the ZM241385 treatment group. The structural damage and decreased organ function induced by Iso was rescued by spironolactone treatment, but was abrogated by pharmacological inactivation of A2AR. The results indicate that A2AR, but not adenosine, is involved in the process of EndMT-driven cardiorenal fibrosis. We propose that these beneficial effects of spironolactone are, at least in part, because of A2AR activation-mediated EndMT inhibition. Our present study does not, however, explain the signaling pathway involved in the A2AR modulation of EndMT.

Studies have demonstrated that adenosine levels increase [33], but A2AR levels decrease [34,35] in the failing heart and kidney. We found similar results in the Iso-treated rats. However, adenosine expression was not significantly changed after spironolactone treatment. A human double-blinded randomized controlled study reported that eplerenone

does not affect adenosine formation, and that increased levels of extracellular adenosine are unlikely to contribute to the cardioprotective effect of mineralocorticoid receptor antagonists [36].

However, activation of A2AR also produces pro-fibrotic effects. A2AR occupancy stimulated collagen production by hepatic stellate cells, while A2AR-deficient mice or wild-type mice treated with ZM241385 were protected from hepatic fibrosis [37]. Pharmacological blockade of A2AR diminished dermal fibrosis [21]. This phenomenon demonstrates that A2AR plays a different role in cell- and tissue-specific manners [18]. More studies are needed to further explore the molecular mechanism, such as the signaling pathways involved in the A2AR regulation of EndMT.

5. Conclusion

Our study demonstrates that A2AR inhibits EndMT to improve cardiorenal fibrosis after spironolactone treatment of cardiac and renal injury caused by Iso. A2AR may provide a novel therapeutic target for cardiorenal syndrome.

Author contributions

Hao Zhou and Yongsheng Gong designed the experiment. Jie Hu, Lingzhi Chen, Xiaofang Fan, and Wenhua Ge performed experiments. Wenhua Ge, Hao Zhou and Xingxing Chen contributed to data analysis. Xingxing Chen wrote the paper.

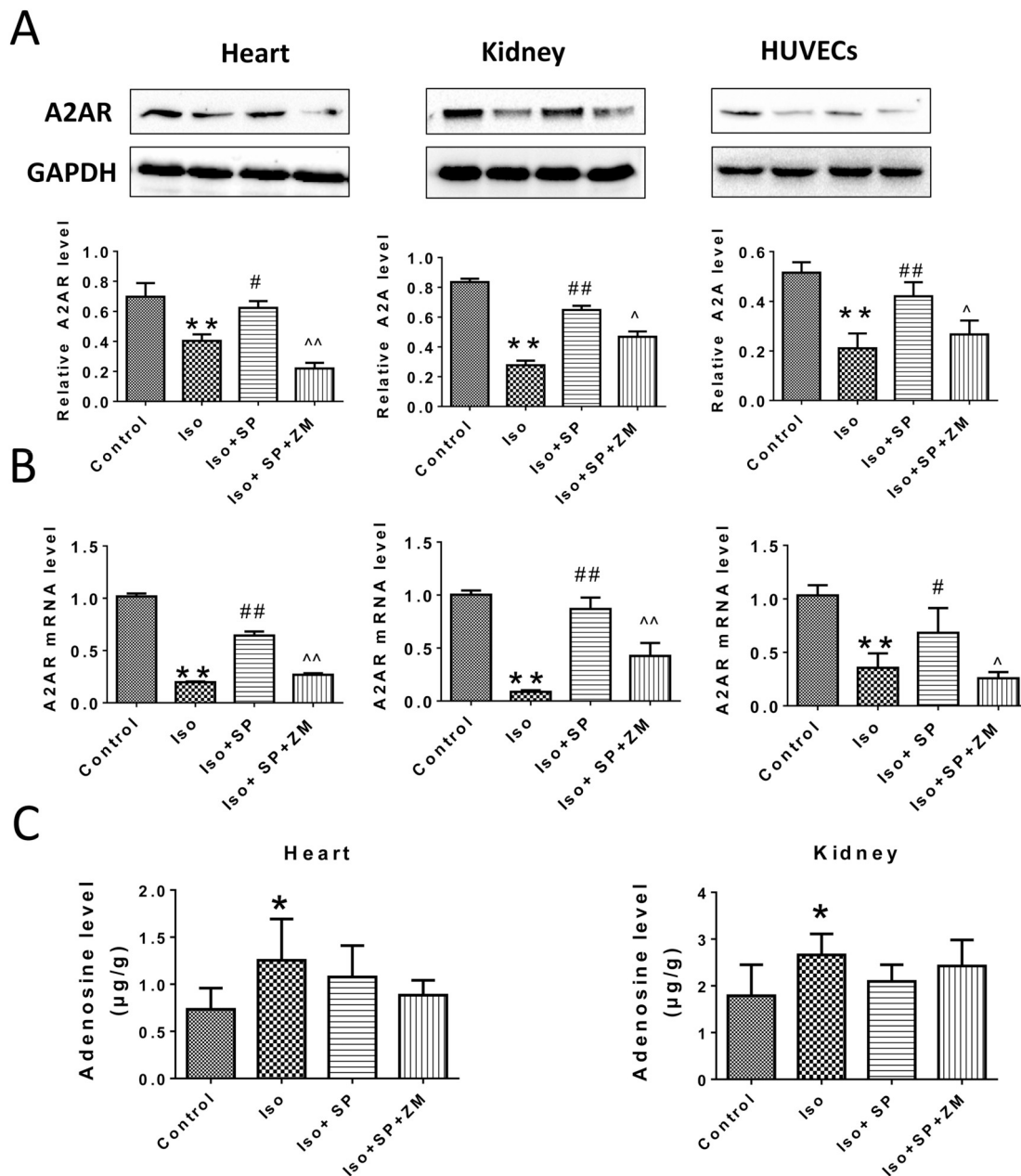


Fig. 6. Expression of A2AR and adenosine levels in cardiac and renal tissues. (A) Western blotting analysis of A2AR, n = 4–6. (B) RT-PCR analysis of A2AR, n = 5–8. (C) UPLC-MS/MS analysis of adenosine level, n = 4. *P < 0.05, **P < 0.01 vs. Control; #P < 0.05, ##P < 0.01 vs. Iso; ^P < 0.05, ^^P < 0.01 vs. Iso + SP.

Table 3
UPLC-MS/MS analysis of adenosine level in heart and kidney.

| Group | No | Heart adenosine (µg/g) | kidney adenosine (µg/g) |
|---------------|----|------------------------|-------------------------|
| Control | 4 | 0.73 ± 0.23 | 1.79 ± 0.66 |
| Iso | 4 | 1.25 ± 0.44* | 2.66 ± 0.45* |
| Iso + SP | 4 | 1.08 ± 0.33 | 2.10 ± 0.35 |
| Iso + SP + ZM | 4 | 0.88 ± 0.16 | 2.43 ± 0.56 |

Data shown as mean ± standard deviation.
* P < 0.05 vs. Control.

Acknowledgments

This research was supported by the National Natural Science Foundation of China [grant number: 81570364; 81873468], and the Science and Technology Planning Project of Wenzhou Science and Technology Bureau of Zhejiang Province of China [grant number:

Y20150032; Y20170021], and in part by the Foundation for the Program of the Provincial Health Department of Zhejiang Province of China [grant number: 2019RC051].

Disclosure statement

The authors confirm that there are no conflicts of interest.

Appendix A. Supplementary data

Supplementary data to this article can be found online at <https://doi.org/10.1016/j.lfs.2019.01.017>.

References

[1] C. Ronco, P. McCullough, S.D. Anker, I. Anand, N. Aspromonte, S.M. Bagshaw, R. Bellomo, T. Berl, I. Bobek, D.N. Cruz, L. Daliento, A. Davenport, M. Haapio,

- H. Hillege, A.A. House, N. Katz, A. Maisel, S. Mankad, P. Zanco, A. Mebazaa, A. Palazzuoli, F. Ronco, A. Shaw, G. Sheinfeld, S. Soni, G. Vescovo, N. Zamperetti, P. Ponikowski, Cardio-renal syndromes: report from the consensus conference of the acute dialysis quality initiative, *Eur. Heart J.* 31 (2010) 703–711, <https://doi.org/10.1093/eurheartj/ehp507>.
- [2] A.I. Löffler, T.P. Cappola, J. Fang, S.J. Hetzel, A. Kadlec, B. Astor, N.K. Sweitzer, Effect of renal function on prognosis in chronic heart failure, *Am. J. Cardiol.* 115 (2015) 62–68, <https://doi.org/10.1016/j.amjcard.2014.09.055>.
- [3] J.P. Granger, Maternal and fetal adaptations during pregnancy: lessons in regulatory and integrative physiology, *Am. J. Phys. Regul. Integr. Comp. Phys.* 301 (2002) R267–R275, <https://doi.org/10.1152/ajpregu.00562.2002>.
- [4] J.R. Teerlink, G. Cotter, B.A. Davison, G.M. Felker, G. Filippatos, B.H. Greenberg, P. Ponikowski, E. Unemori, A.A. Voors, K.F. Adams, M.I. Dorobantu, L.R. Grinfeld, G. Jondeau, A. Marmor, J. Masip, P.S. Pang, K. Werdan, S.L. Teichman, A. Trapani, C.A. Bush, R. Saini, C. Schumacher, T.M. Severin, M. Metra, Serelaxin, recombinant human relaxin-2, for treatment of acute heart failure (RELAX-AHF): a randomised placebo-controlled trial, *Lancet* 381 (2013) 29–39, [https://doi.org/10.1016/S0140-6736\(12\)61855-8](https://doi.org/10.1016/S0140-6736(12)61855-8).
- [5] M. Metra, G. Cotter, B.A. Davison, G.M. Felker, G. Filippatos, B.H. Greenberg, P. Ponikowski, E. Unemori, A.A. Voors, K.F. Adams, M.I. Dorobantu, L. Grinfeld, G. Jondeau, A. Marmor, J. Masip, P.S. Pang, K. Werdan, M.F. Prescott, C. Edwards, S.L. Teichman, A. Trapani, C.A. Bush, R. Saini, C. Schumacher, T. Severin, J.R. Teerlink, Effect of serelaxin on cardiac, renal, and hepatic biomarkers in the relaxin in acute heart failure (RELAX-AHF) development program: correlation with outcomes, *J. Am. Coll. Cardiol.* 61 (2013) 196–206, <https://doi.org/10.1016/j.jacc.2012.11.005>.
- [6] F. Zannad, P. Rossignol, Cardioresenal syndrome revisited, *Circulation* 138 (2018) 929–944, <https://doi.org/10.1161/CIRCULATIONAHA.117.028814>.
- [7] S. Liu, A.R. Kompa, S. Kumfu, F. Nishijima, D.J. Kelly, H. Krum, B.H. Wang, Subtotal nephrectomy accelerates pathological cardiac remodeling post-myocardial infarction: implications for cardioresenal syndrome, *Int. J. Cardiol.* 168 (2013) 1866–1880, <https://doi.org/10.1016/j.ijcard.2012.12.065>.
- [8] D.C. Crawford, A.V. Chobanian, P. Brecher, Angiotensin II induces fibronectin expression associated with cardiac fibrosis in the rat, *Circ. Res.* 74 (1994) 727–739, <https://doi.org/10.1161/01.RES.74.4.727>.
- [9] M.D.M. Cezar, R.L. Damatto, L.U. Pagan, A.R.R. Lima, P.F. Martinez, C. Bonomo, C.M. Rosa, D.H.S. Campos, A.C. Cicogna, M.J. Gomes, S.A. Oliveira, D.A. Blotta, M.P. Okoshi, K. Okoshi, Early spironolactone treatment attenuates heart failure development by improving myocardial function and reducing fibrosis in spontaneously hypertensive rats, *Cell. Physiol. Biochem.* 36 (2015) 1453–1466, <https://doi.org/10.1159/000430310>.
- [10] M. Taira, H. Toba, M. Murakami, I. Iga, R. Serizawa, S. Murata, M. Kobara, T. Nakata, Spironolactone exhibits direct renoprotective effects and inhibits renal renin-angiotensin-aldosterone system in diabetic rats, *Eur. J. Pharmacol.* 589 (2008) 264–267, <https://doi.org/10.1016/j.ejphar.2008.06.019>.
- [11] L. Calvier, E. Martinez-Martinez, M. Miana, V. Cachofeiro, E. Rousseau, J.R. Sádaba, F. Zannad, P. Rossignol, N. López-Andrés, The impact of galectin-3 inhibition on aldosterone-induced cardiac and renal injuries, *JACC Heart Fail.* 3 (2015) 59–67, <https://doi.org/10.1016/j.jchf.2014.08.002>.
- [12] J. Cai, X. Chen, X. Chen, L. Chen, G. Zheng, H. Zhou, X. Zhou, Anti-fibrosis effect of relaxin and spironolactone combined on isoprenaline-induced myocardial fibrosis in rats via inhibition of endothelial-mesenchymal transition, *Cell. Physiol. Biochem.* 41 (2017) 1167–1178, <https://doi.org/10.1159/000464125>.
- [13] F. Rieder, S.P. Kessler, G.A. West, S. Bhilocha, C. De La Motte, T.M. Sadler, B. Gopalan, E. Stylianou, C. Fiocchi, Inflammation-induced endothelial-to-mesenchymal transition: a novel mechanism of intestinal fibrosis, *Am. J. Pathol.* 179 (2011) 2660–2673, <https://doi.org/10.1016/j.ajpath.2011.07.042>.
- [14] J. He, Y. Xu, D. Koya, K. Kanasaki, Role of the endothelial-to-mesenchymal transition in renal fibrosis of chronic kidney disease, *Clin. Exp. Nephrol.* 17 (2013) 488–497, <https://doi.org/10.1007/s10157-013-0781-0>.
- [15] E.M. Zeisberg, O. Tarnavski, M. Zeisberg, A.L. Dorfman, J.R. McMullen, E. Gustafsson, A. Chandraker, X. Yuan, W.T. Pu, A.B. Roberts, E.G. Neilson, M.H. Sayegh, S. Izumo, R. Kalluri, Endothelial-to-mesenchymal transition contributes to cardiac fibrosis, *Nat. Med.* 13 (2007) 952–961, <https://doi.org/10.1038/nm1613>.
- [16] S. Piera-Velazquez, F. Mendoza, S. Jimenez, Endothelial to mesenchymal transition (EndoMT) in the pathogenesis of human fibrotic diseases, *J. Clin. Med.* 5 (2016), <https://doi.org/10.3390/jcm5040045> (pii: E45).
- [17] K. Schmidt, R. Tissier, B. Ghaleh, T. Drogies, S.B. Felix, T. Krieg, Cardioprotective effects of mineralocorticoid receptor antagonists at reperfusion, *Eur. Heart J.* 31 (2010) 1655–1662, <https://doi.org/10.1093/eurheartj/ehp555>.
- [18] S. Kazerounian, K.O. Yee, J. Lawler, Thrombospondins in cancer, *Cell. Mol. Life Sci.* 64 (2008) 1471–1483, <https://doi.org/10.1007/s00018-007-7486-z>.
- [19] E.A. Hamad, W. Zhu, T.O. Chan, V. Myers, E. Gao, X. Li, J. Zhang, J. Song, X.Q. Zhang, J.Y. Cheung, W. Koch, A.M. Feldman, Cardioprotection of controlled and cardiac-specific over-expression of a2A-adenosine receptor in the pressure overload, *PLoS One* 7 (2012) e39919, <https://doi.org/10.1371/journal.pone.0039919>.
- [20] G.E. Garcia, L.D. Truong, J.F. Chen, R.J. Johnson, L. Feng, Adenosine A2A receptor activation prevents progressive kidney fibrosis in a model of immune-associated chronic inflammation, *Kidney Int.* 80 (2011) 378–388, <https://doi.org/10.1038/ki.2011.101>.
- [21] M. Perez-Aso, A. Mediero, Y.C. Low, J. Levine, B.N. Cronstein, Adenosine A2A receptor plays an important role in radiation-induced dermal injury, *FASEB J.* 30 (2016) 457–465, <https://doi.org/10.1096/fj.15-280388>.
- [22] H. Xiao, H.Y. Shen, W. Liu, R. ping Xiong, P. Li, G. Meng, N. Yang, X. Chen, L.Y. Si, Y.G. Zhou, Adenosine A2A receptor: a target for regulating renal interstitial fibrosis in obstructive nephropathy, *PLoS One* 8 (2013) e60173, <https://doi.org/10.1371/journal.pone.0060173>.
- [23] J. Cheng, H. Jin, X. Hou, J. Lv, X. Gao, G. Zheng, Disturbed tryptophan metabolism correlating to progression and metastasis of esophageal squamous cell carcinoma, *Biochem. Biophys. Res. Commun.* 486 (2017) 781–787, <https://doi.org/10.1016/j.bbrc.2017.03.120>.
- [24] P. Hatamizadeh, G.C. Fonarow, M.J. Budoff, S. Darabian, C.P. Kovesdy, K. Kalantar-Zadeh, Cardioresenal syndrome: pathophysiology and potential targets for clinical management, *Nat. Rev. Nephrol.* 9 (2013) 99–111, <https://doi.org/10.1038/nrneph.2012.279>.
- [25] D.C. Rockey, P.D. Bell, J.A. Hill, Fibrosis - a common pathway to organ injury and failure, *N. Engl. J. Med.* 372 (2015) 1138–1149, <https://doi.org/10.1056/NEJMr1300575>.
- [26] A. Struthers, H. Krum, G.H. Williams, A comparison of the aldosterone-blocking agents eplerenone and spironolactone, *Clin. Cardiol.* 31 (2008) 153–158, <https://doi.org/10.1002/clc.20324>.
- [27] A. Capuano, C. Scavone, C. Vitale, L. Sportiello, F. Rossi, G.M.C. Rosano, A.J.S. Coats, Mineralocorticoid receptor antagonists in heart failure with preserved ejection fraction (HFpEF), *Int. J. Cardiol.* 200 (2015) 15–19, <https://doi.org/10.1016/j.ijcard.2015.07.038>.
- [28] X. Huang, Y. He, Y. Chen, P. Wu, D. Gui, H. Cai, A. Chen, M. Chen, C. Dai, D. Yao, L. Wang, Baicalin attenuates bleomycin-induced pulmonary fibrosis via adenosine A2a receptor related TGF- β 1-induced ERK1/2 signaling pathway, *BMC Pulm. Med.* 16 (2016) 132, <https://doi.org/10.1186/s12890-016-0294-1>.
- [29] L.M. Kreckler, E. Gizewski, T.C. Wan, J.A. Auchampach, Adenosine suppresses lipopolysaccharide-induced tumor necrosis factor- α production by murine macrophages through a protein kinase A- and exchange protein activated by cAMP-independent signaling pathway, *J. Pharmacol. Exp. Ther.* 331 (2009) 1051–1061, <https://doi.org/10.1124/jpet.109.157651>.
- [30] M.G. Seidel, M. Klinger, M. Freissmuth, C. Holler, Activation of mitogen-activated protein kinase by the A(2A)-adenosine receptor via a rap1-dependent and via a p21(ras)-dependent pathway, *J. Biol. Chem.* 274 (1999) 25833–25841, <https://doi.org/10.1074/jbc.M100166-01>.
- [31] M. Zuccarini, P. Giuliani, S. Buccella, V. Di Liberto, G. Mudò, N. Belluardo, M. Carluccio, M. Rossini, D.F. Condorelli, M.P. Rathbone, F. Caciagli, R. Ciccarelli, P. Di Iorio, Modulation of the TGF- β 1-induced epithelial to mesenchymal transition (EMT) mediated by P1 and P2 purine receptors in MDCK cells, *Purinergic Signal* 13 (2017) 429–442, <https://doi.org/10.1007/s11302-017-9571-6>.
- [32] M. Perez-Aso, A. Mediero, B.N. Cronstein, Adenosine A2A receptor (A2AR) is a fine-tune regulator of the collagen1: collagen3 balance, *Purinergic Signal* 9 (2013) 573–583, <https://doi.org/10.1007/s11302-013-9368-1>.
- [33] H. Funaya, M. Kitakaze, K. Node, T. Minamino, K. Komamura, M. Hori, Plasma adenosine levels increase in patients with chronic heart failure, *Circulation* 95 (1997) 1363–1365, <https://doi.org/10.1161/01.cir.95.6.1363>.
- [34] M. Asakura, H. Asanuma, J. Kim, Y. Liao, K. Nakamaru, M. Fujita, K. Komamura, T. Isomura, H. Furukawa, H. Tomoike, M. Kitakaze, Impact of adenosine receptor signaling and metabolism on pathophysiology in patients with chronic heart failure, *Hypertens. Res.* 30 (2007) 781–787, <https://doi.org/10.1291/hyres.30.781>.
- [35] H.T. Lee, C.W. Emala, Systemic adenosine given after ischemia protects renal function via A2adenosine receptor activation, *Am. J. Kidney Dis.* 38 (2001) 610–618, <https://doi.org/10.1053/ajkd.2001.26888>.
- [36] T.N.A. Van Den Berg, J. Deinum, A. Bilos, A.R.T. Donders, G.A. Rongen, N.P. Riksen, The effect of eplerenone on adenosine formation in humans in vivo: a double-blinded randomised controlled study, *PLoS One* 9 (2014) e111248, <https://doi.org/10.1371/journal.pone.0111248>.
- [37] E.S.L. Chan, M.C. Montesinos, P. Fernandez, A. Desai, D.L. Delano, H. Yee, A.B. Reiss, M.H. Pillinger, J.F. Chen, M.A. Schwarzschild, S.L. Friedman, B.N. Cronstein, Adenosine A2A receptors play a role in the pathogenesis of hepatic cirrhosis, *Br. J. Pharmacol.* 148 (2006) 1144–1155, <https://doi.org/10.1038/sj.bjp.0706812>.